Two-nucleon spectroscopic amplitudes associated with pairing vibrational modes in closed-shell systems

$\boxed{box\ 3}$ I

App. 2C

The solution of the pairing Hamiltonian

$$H = H_{sp} + H_p ,$$

where

$$H_{sp} = \sum_\nu \varepsilon_\nu a^\dagger_\nu a_\nu$$

and

$$H_p = -G P^\dagger P ,$$

with

$$P^\dagger = \sum_{\nu>0} a^\dagger_\nu a^\dagger_{\tilde\nu} ,$$

in the Harmonic approximation (RPA) leads to pair addition (a)/a pair removal (r) two-particle, two-hole correlated modes, the associated creation and annihilation operators being

$$\Gamma^\dagger_a(n) = \sum_k X^a_n(k)\,\Gamma^\dagger_k + \sum_i Y^a_n(i)\,\Gamma_i$$

and

$$\Gamma^\dagger_r(n) = \sum_i X^r_n(i)\,\Gamma^\dagger_i + \sum_k Y^r_n(k)\,\Gamma_k ,$$

with

$$\sum X^2 - \sum Y^2 = 1$$

and

$$\Gamma^\dagger_k = a^\dagger_k a^\dagger_{\tilde k} , \qquad (\varepsilon_k > \varepsilon_F),$$

$$\Gamma^\dagger_i = a_{\tilde i}\, a_i . \qquad (\varepsilon_k \le \varepsilon_F).$$

The relations

$$[H, \Gamma^\dagger_a(n)] = \hbar W_n \,(\beta = +2)$$

(and

box 3 cont. II

$$[H, \Gamma_r^\dagger(n)] = \hbar W_n(\beta=-2),$$

where β is the transfer quantum, while n labels the roots of the corresponding dispersion relations

$$\frac{1}{G(\pm 2)} = \sum_k \frac{\pm(\Omega_k/2)}{2\epsilon_k \mp W_n(\pm 2)} + \sum_i \frac{(\Omega_i/2)}{2\varepsilon_i \pm W_n(\pm 2)}$$

in increasing order of energy.

For the case of the (neutron) pair addition and pair substraction modes of ^{208}Pb the above equation can be graphically solved (cf. Fig. 1), the minimum of the dispersion relation coincides with the Fermi energy.

One then obtains

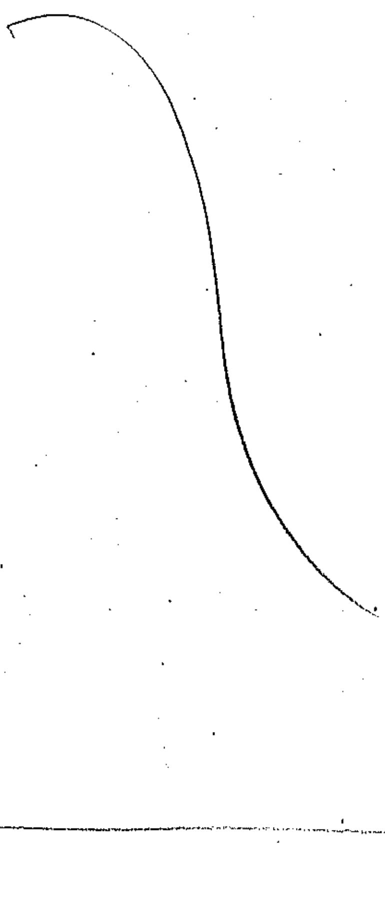

Box 3

III

4.17
-1.248
2.922

$W_1(-2)+W_1(+2)$
$= 4.995$ MeV

2.65
-0.64
2.01

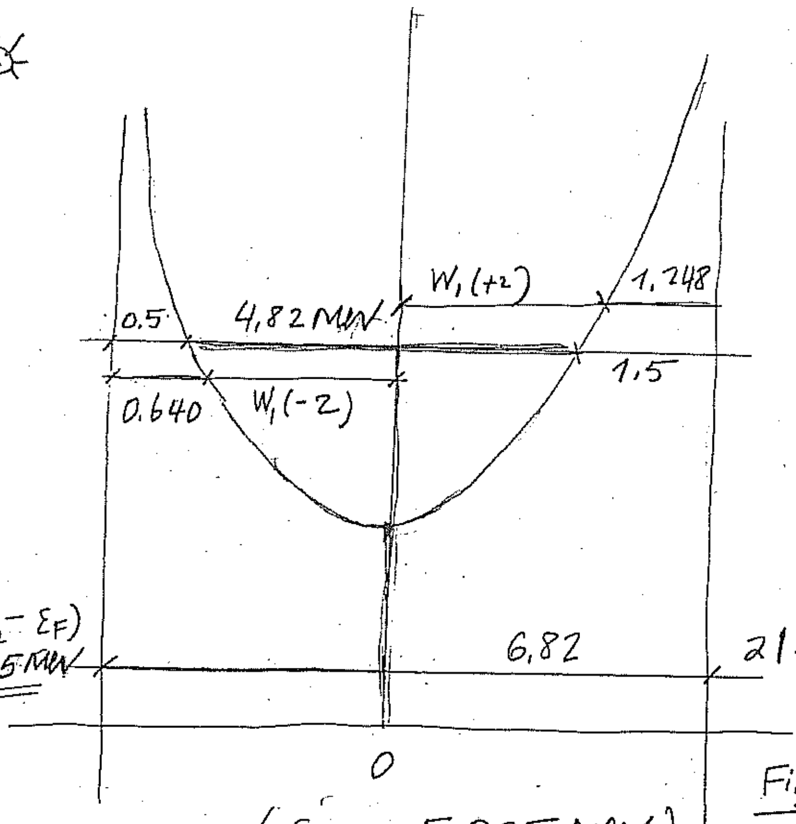

Fig. 1

$(\varepsilon_F = -5.825$ MeV$)$

$$\begin{cases} E_{corr}(+2) = B(208) + B(210) - 2B(209) = 1.248 \text{ MeV} \\ E_{corr}(-2) = B(208) + B(206) - 2B(207) = 0.630 \text{ MeV} \end{cases}$$

$$W_1(+2) + W_1(-2) = (B(208) - B(206)) - (B(210) - B(208))$$

$(\varepsilon_{p1/2} - \varepsilon_{g9/2} = 3.41$ MeV$)$ $= 14.110 - 9.115 = 4.995$ MeV

orbit	ε_j	$\lvert\varepsilon_{p1/2} - \varepsilon_k\rvert = \lvert\varepsilon_k\rvert - \lvert\varepsilon_{p1/2}\rvert$
$0h_{9/2}$	-10.62	3.47
$1f_{7/2}$	-9.50	2.35
$0i_{13/2}$	-8.79	1.64
$2p_{3/2}$	-8.05	0.90
$1f_{5/2}$	-7.72	0.57
$2p_{1/2}$	-7.15	3.01
$\varepsilon_F = -5.825$ MeV		$\varepsilon_k - \varepsilon_{g9/2} = \lvert\varepsilon_{g9/2}\rvert - \lvert\varepsilon_k\rvert$
$1g_{9/2}$	-3.74	0
$0i_{11/2}$	-2.97	0.77
$0j_{15/2}$	-2.33	1.41
$2d_{5/2}$	-2.18	1.56
$3s_{1/2}$	-1.71	2.03
$1g_{7/2}$	-1.27	2.47
$2d_{3/2}$	-1.23	2.51

From Fig. 2.C.1

$$2(\varepsilon_{g9/2} - \varepsilon_F) = W_1(+2) + E_{corr}(+2)$$

$4.17 \text{ MeV} = 2(-3.74 - (-5.825)) = W_1(+2) + 1.248$ MeV

Thus $W_1(+2) = 2.922$ MeV

$$2(\varepsilon_F - \varepsilon_{p1/2}) = W_1(-2) + E_{corr}(-2)$$

$2.65 \text{ MeV} = 2(-5.825 - (-7.15))$ MeV $= W_1(-2) + 0.640$ MeV

Thus $W_1(-2) = 2.01$ MeV $W_1(+2) + W_1(-2) = 4.93$ MeV

Let us make a rigid shift in energies setting $\varepsilon_F = 0$, Thus

$$\begin{cases} W_1(+2) = 2\varepsilon_{g9/2} - E_{corr}(2) \\ W_1(-2) = -2\varepsilon_{p1/2} - E_{corr}(-2) \end{cases}$$

All energies >0, i.e ε_F Luca Vago   (2) Box 3

$$\varepsilon_i \le \varepsilon_F \Rightarrow \underline{\varepsilon_F - \varepsilon_i} = -|\varepsilon_F| + |\varepsilon_i| = |\varepsilon_i| - |\varepsilon_F| > 0$$

$$\varepsilon_k > \varepsilon_F \qquad \underline{\varepsilon_k - \varepsilon_F} = -|\varepsilon_k| + |\varepsilon_F| = |\varepsilon_F| - |\varepsilon_k| > 0$$

$$\left\{ \begin{aligned} 2(\varepsilon_F - \varepsilon_{p1/2}) &= \overset{>0}{W_1(-2)} + \overset{>0}{E_{corr}(-2)} > 0 \\ 2(\varepsilon_{g9/2} - \varepsilon_F) &= \overset{>0}{W_1(+2)} + \overset{>0}{E_{corr}(+2)} > 0 \end{aligned} \right\}$$

$\boxed{\text{Pair substraction mode}}$

$$X_1^r(i) = \frac{\frac{1}{2}\Omega_i^{1/2}\Lambda_1(-2)}{2(\varepsilon_F - \varepsilon_i) - W_1(-2)}$$

$$2(\varepsilon_F - \varepsilon_i) - W_1(-2) = 2(\cancel{\varepsilon_F} - \varepsilon_i) - \left(2(\cancel{\varepsilon_F} - \varepsilon_{p1/2}) - E_{corr}(-2)\right)$$

$$= 2(\varepsilon_{p1/2} - \varepsilon_i) + E_{corr}(-2) = 2(|\varepsilon_i| - |\varepsilon_{p1/2}|) + E_{corr}(-2)$$

$$\boxed{X_1^r(i) = \frac{\frac{1}{2}\Omega_i^{1/2}\Lambda_1(-2)}{2(|\varepsilon_i| - |\varepsilon_{p1/2}|) + E_{corr}(-2)}} \qquad \boxed{X_1^r(i) = \frac{\frac{1}{2}\Omega_i^{1/2}\Lambda_1(-2)}{2(|\varepsilon_i| - |\varepsilon_{p1/2}|) + 0.640\ \text{MeV}}}$$

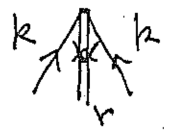

$$Y_1^r(k) = -\frac{\frac{1}{2}\Omega_k^{1/2}\Lambda_1(-2)}{2(\varepsilon_k - \varepsilon_F) + W_1(-2)}$$

$$2(\varepsilon_k - \cancel{\varepsilon_F}) + 2(\cancel{\varepsilon_F} - \varepsilon_{p1/2}) - E_{corr}^{(-2)} = 2(\varepsilon_k - \varepsilon_{p1/2}) - E_{corr}(-2)$$

$$= 2(|\varepsilon_{p1/2}| - |\varepsilon_k|) - E_{corr}(-2) = 2\overbrace{(|\varepsilon_{p1/2}| - |\varepsilon_{g9/2}|)}^{\text{single-particle en. gaps}}$$

$$+ 2(|\varepsilon_{g9/2}| - |\varepsilon_k|) - E_{corr}(-2)$$

$$Y_1^r(k) = -\frac{\frac{1}{2}\Omega_k^{1/2}\Lambda_1(-2)}{2(|\varepsilon_{g9/2}| - |\varepsilon_k|) + 2\underbrace{(|\varepsilon_{p1/2}| - |\varepsilon_{g9/2}|)}_{6.82\ \text{MeV}} - \underbrace{E_{corr}(-2)}_{0.640\ \text{MeV}}}$$

$$\boxed{Y_1^r(k) = \frac{\frac{1}{2}\Omega_k^{1/2}\Lambda_1(-2)}{2(|\varepsilon_{g9/2}| - |\varepsilon_k|) + 6.18\ \text{MeV}}}$$

Box3 (3)

$$X_1^r(i) = \frac{\frac{1}{2}\Omega_i^{1/2}\Lambda_1(-2)}{2(|\varepsilon_i|-|\varepsilon_{p1/2}|)+E_{corr}(-2)} \;;\; Y_1^r(k) = \frac{\frac{1}{2}\Omega_k^{1/2}\Lambda_1(-2)}{2(|\varepsilon_{g9/2}|-|\varepsilon_k|) + 2(|\varepsilon_{p1/2}|-|\varepsilon_{g9/2}|) - E_{corr}(-2)}$$

$E_{corr}(-2) = 0.5$ MeV (cf. Fig. 1) $\quad \Omega = j + 1/2$

$2(|\varepsilon_{p1/2}| - |\varepsilon_{g9/2}|) = 6.82$ MeV $\quad 2(|\varepsilon_{p1/2}|-|\varepsilon_{g9/2}|) - E_{corr} = (6.82 - 0.5)$ MeV $= 6.32$ MeV

Thus

$$\begin{cases} X_1^r(i) = \dfrac{\frac{1}{2}\Omega_i^{1/2}\Lambda_1(-2)}{2(|\varepsilon_i|-|\varepsilon_{p1/2}|)+0.5\,\text{MeV}} ; \\[2ex] Y_1^r(k) = -\dfrac{\frac{1}{2}\Omega_k^{1/2}\Lambda_1(-2)}{2(|\varepsilon_{g9/2}|-|\varepsilon_k|)+6.23\,\text{MeV}} \end{cases}$$

Table 2.C.1

units		MeV	MeV^{-1}		TDA
nlj	Ω_i	$\lvert\varepsilon_i\rvert - \lvert\varepsilon_{p1/2}\rvert$	$A(i) = \frac{\frac{1}{2}\Omega_i^{1/2}}{2(\lvert\varepsilon_i\rvert - \lvert\varepsilon_{p1/2}\rvert)+0.5\,\text{MeV}}$	$X_1^r(i)$	$X_1^r(i)$
$2p_{1/2}$	1	0	1	0.83	0.80
$1f_{5/2}$	3	0.57	0.528	0.44	0.42
$2p_{3/2}$	2	0.90	0.307	0.25	0.25
$0i_{13/2}$	7	1.64	0.350	0.29	0.28
$1f_{7/2}$	4	2.35	0.192	0.16	0.15
$0h_{9/2}$	5	3.47	0.150	0.12	0.12

$\sum A^2(i) = 1.5549$ $\quad$ Very similar to column labeled 266 p. Table XVI Adv. NP $\quad \frac{1}{\sqrt{1.5549}} = 0.802 \leftarrow \sum (X_1^r(i)^2)^{TD} = 1$

units		$\lvert\varepsilon\rvert$ MeV	MeV^{-1}	
nlj	Ω_k	$\lvert\varepsilon_{g9/2}\rvert - \lvert\varepsilon_k\rvert$	$B(k) = \frac{\frac{1}{2}\Omega_k\,\Lambda_1(-2)}{2(\lvert\varepsilon_{g9/2}\rvert-\lvert\varepsilon_k\rvert)+6.23\,\text{MeV}}$	$Y_1^r(i)$
$1g_{9/2}$	5	0	0.179	−0.15
$0i_{11/2}$	6	0.77	0.158	−0.13
$0j_{15/2}$	8	1.41	0.156	−0.13
$2d_{5/2}$	3	1.56	0.093	−0.08
$3s_{1/2}$	1	2.03	0.046	−0.04
$1g_{7/2}$	4	2.47	0.090	−0.07
$2d_{3/2}$	2	2.51	0.063	−0.05

$\sum B^2(k) = 0.10418$

$\Lambda_1(-2) = 0.83025$ MeV $\quad \Lambda_1^2(-2)\left(\sum_i A^2(i) - \sum_k B^2(k)\right) = \Lambda_1^2(-2)\,(1.5549 - 0.10418)$

$= \Lambda_1^2(-2)\; 1.45073 = 1$

all energies which enter X, Y are positive

(4)

Box 3

$$W_1(+2) = 2(\varepsilon_{g9/2} - \varepsilon_F) - E_{corr}(+2)$$

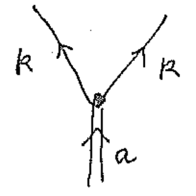

$$X_1^a(k) = \frac{\frac{1}{2}\Omega_k^{1/2}\Lambda_1(+2)}{2(\varepsilon_k - \varepsilon_F) - W_1(+2)}$$

$$2(\varepsilon_k - \varepsilon_F) - W_1(+2) =$$

$$= 2(\varepsilon_k - \cancel{\varepsilon_F}) - \left(2(\varepsilon_{g9/2} - \cancel{\varepsilon_F}) - E_{corr}(+2)\right)$$

$$= 2(\varepsilon_k - \varepsilon_{g9/2}) + E_{corr}(+2)$$

$$= 2(|\varepsilon_{g9/2}| - |\varepsilon_k|) + E_{corr}(+2)$$

$$\boxed{X_1^a(k) = \frac{\frac{1}{2}\Omega_k^{1/2}\Lambda_1(+2)}{2(|\varepsilon_{g9/2}| - |\varepsilon_k|) + E_{corr}(+2)}}$$

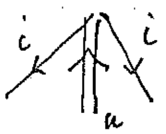

$$Y_1^a(i) = -\frac{\frac{1}{2}\Omega_i^{1/2}\Lambda_1(+2)}{2(\varepsilon_F - \varepsilon_i) + W_1(+2)}$$

$$2(\varepsilon_F - \varepsilon_i) + W_1(+2) = 2(\cancel{\varepsilon_F} - \varepsilon_i) + 2(\varepsilon_{g9/2} - \cancel{\varepsilon_F}) - E_{corr}(+2)$$

$$= 2(\varepsilon_{p1/2} - \varepsilon_i) + 2(\varepsilon_{g9/2} - \varepsilon_{p1/2}) - E_{corr}(+2)$$

$$= 2(|\varepsilon_i| - |\varepsilon_{p1/2}|) + \underbrace{2\,\underbrace{(|\varepsilon_{p1/2}| - |\varepsilon_{g9/2}|)}_{\text{s.p. gap } 3.41\,\text{MeV}}}_{6.28\,\text{MeV}} - \underbrace{E_{corr}(+2)}_{1.248\,\text{MeV (see Fig. 1)}}$$

~~ansatz~~ ~~$E_{corr}(+2) = 1.5$ MeV~~

OK $\boxed{\cancel{Y_1^a(i) = -\frac{\frac{1}{2}\Omega_i^{1/2}\Lambda_1(+2)}{2(|\varepsilon_i| - |\varepsilon_{p1/2}|) + 5.032\,\text{MeV}}}}$

$$\boxed{Y_1^a(i) = -\frac{\frac{1}{2}\Omega_i^{1/2}\Lambda_1(+2)}{2(|\varepsilon_i| - |\varepsilon_{p1/2}|) + 2\Delta\varepsilon_{sp} - E_{corr}(+2)}}$$

$\Delta\varepsilon_{sp}$ = single-particle closed shell gap > 0

$E_{corr}(+2) = 1.5$ MeV (conf. Fig. 1) Box 3

$\Delta\varepsilon_{sp} = 2\left(|\varepsilon_{p1/2}| - |\varepsilon_{g9/2}|\right) = 6.82$ MeV

Thus $2\Delta\varepsilon_{sp} - E_{corr} = (6.82 - 1.5)$ MeV $= 5.32$ MeV

$$\begin{cases} X_1^a(k) = \dfrac{\frac{1}{2}\Omega_k^{1/2}\,\Lambda_1(+2)}{2(|\varepsilon_{g9/2}| - |\varepsilon_k|) + 1.5\text{ MeV}} \\[2ex] Y_1^a(i) = -\dfrac{\frac{1}{2}\Omega_i^{1/2}\,\Lambda_1(+2)}{2(|\varepsilon_i| - |\varepsilon_{p1/2}|) + 5.32\text{ MeV}} \end{cases} \qquad \Omega_j = \frac{2j+1}{2}$$

Table 2.C.2

Units		MeV	MeV^{-1}	
$n l_k j_k$	Ω_k	$\lvert\varepsilon_{g9/2}\rvert - \lvert\varepsilon_k\rvert$	$C(k) = \dfrac{\frac{1}{2}\Omega_k^{1/2}}{2(\lvert\varepsilon_{g9/2}\rvert - \lvert\varepsilon_k\rvert) + 1.5\text{ MeV}}$	$X_1^a(k)$
$1g_{9/2}$	5	0	0.745	0.82
$0i_{11/2}$	6	0.77	0.403	0.44
$0j_{15/2}$	8	1.41	0.327	0.36
$2d_{5/2}$	3	1.56	0.187	0.21
$3s_{1/2}$	1	2.03	0.090	0.10
$1g_{7/2}$	4	2.47	0.155	0.17
$2d_{3/2}$	2	2.51	0.108	0.12

$\sum_k C^2(k) = 0.903$

coincides exactly with column labelled ^{210}Pb of Table XVI Adv. in N.P.

Units		MeV	MeV^{-1}	
$n l_i j_i$	Ω_i	$\lvert\varepsilon_i\rvert - \lvert\varepsilon_{p1/2}\rvert$	$D(i) = -\dfrac{\frac{1}{2}\Omega_i^{1/2}}{2(\lvert\varepsilon_i\rvert - \lvert\varepsilon_{p1/2}\rvert) + 5.32\text{ MeV}}$	$Y_1^a(i)$
$2p_{1/2}$	1	0	-0.094	-0.10
$1f_{5/2}$	3	0.57	-0.134	-0.15
$2p_{3/2}$	2	0.90	-0.099	-0.11
$0i_{13/2}$	7	1.64	-0.154	-0.17
$1f_{7/2}$	4	2.35	-0.100	-0.11
$0h_{9/2}$	5	3.47	-0.091	-0.10

$\sum_i D^2(i) = 0.079$

$\Lambda_1^2(+2)\left(\sum_k C^2(k) - \sum_i D^2(i)\right) = (0.903 - 0.079)\text{ MeV}^{-2} = 0.824\text{ MeV}^{-2}$; $\Lambda_1(+2) = \dfrac{\text{MeV}}{\sqrt{0.824}} = 1.102$ MeV

$\Lambda_1(+2) = 1.102$ MeV

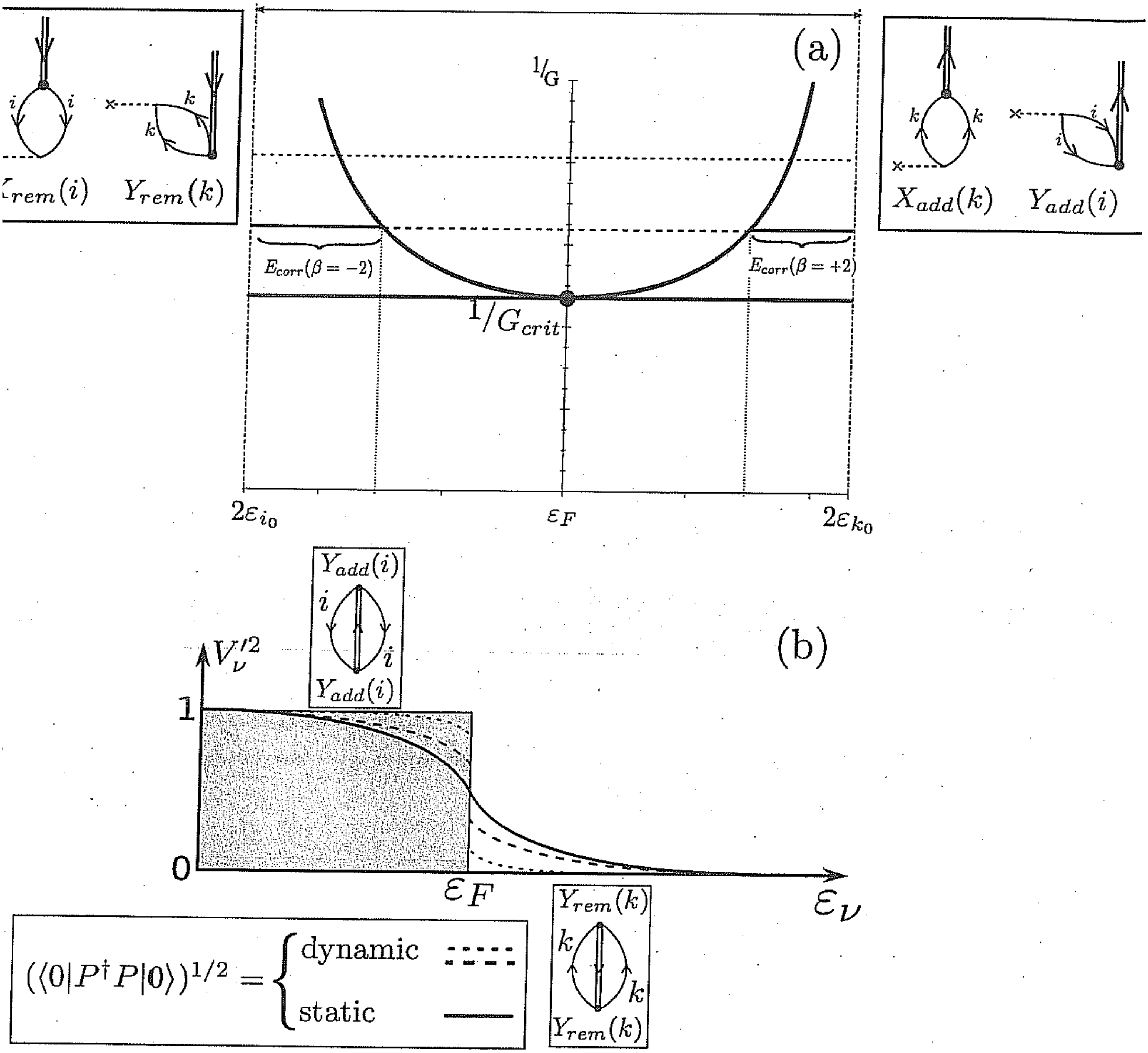

Fig. 2.C.2

~~Fig. 2 Box 3~~

Fig. 2.C.2

Schematic reresentation of the quantal phase transition taking place as function of the pairing coupling constant in a (model) closed shell nucleus. **(a)** dispersion relation associated with the RPA diagonalization of the Hamiltonian $H = H_{sp} + H_p$ for the pair addition and pair removal modes. In the inset are shown the two-particle transfer processes exciting these modes, which testify to the fact that the associated zero point fluctuations (ZPF) which diverge at $G = G_{crit}$, blur the distinction between occupied and empty states typical of closed shell nuclei. **(b)** occupation number associated with the single-particle levels. For $G < G_{crit}$ there is a dynamical depopulation (population) of levels i (k) below (above) the Fermi energy. For $G \geq G_{crit}$, the deformation of the Fermi surface becomes static, although with a consistent dynamic component. In fact, the actual value of the pairing gap is $\Delta = \sqrt{\Delta^2_{BCS} + 1/2\, G^2 S_0(RPA)}$, (cf. e.g. Brink and Broglia, Ch. 6), where $S_0(RPA) = \sum_{n \neq AGN} \left[|\langle n|P|0\rangle|^2 + \langle n|P^\dagger|0\rangle|^2\right]_{RPA}$, where $\Delta_{BCS} = G|\langle BCS|P^\dagger|BCS\rangle|$ is the standard, static BCS pairing gap, while G is the pairing force strength. The non-energy weighted sum rule $S_0(RPA)$ describes the contribution of pairing fluctuations, to the effective (RPA) gap. and is intimately associated with projection in particle number. It is of notice that $\sum_{n \neq AGN}$ means that the divergent contribution from the zero energy mode (Anderson, Goldstone, Nambu mode), associated with the lowest ($\hbar\omega 0$) solution of the $H = H_{sp} + H''_p$ (cf. Brink and Broglia App. J) is to be excluded (cf. also Shimizu et al. (1989) Rev. Mod. Phys. **61**:131).

($\hbar\omega = 0$)

Microscopic mechanism to break gauge invariance

~~box 4~~ (1)

App. 2.D

Pairing is intimately connected with particle number violation and thus spontaneous breaking of gauge invariance, as testified by the order parameter $\langle BCS|P^{+}|BCS\rangle = \alpha_0$. Now, in the nuclear case and at variance with condensed matter, dynamical breaking of gauge symmetry is equally important (pairing vibrations around closed shell nuclei, cf. Fig. 2 box 3). The fact that the average single-particle field acts as an external potential (like e.g. magnetic field in metallic superconductors) is at the basis of of the existence of a critical value of the pairing strength G to bind Cooper pairs in nuclei. In fact, spatial quantization in finite systems at large and in nuclei in particular, intimately connecte with the paramount role the surface has in these systems, is at the basis of the existence of a critical G value. Also of the fact that in nuclei an important fraction (30-50%) of Cooper pair binding is due to the exchange of collective vibrations between the partners of the pair, the rest being associated with the bare NN interaction in the $^1S_0$ channel (cf. Fig. 1)

Now, there are situations in which spatial quantization screens, essentially completely, the NN-interaction. This happens in the case in which the nuclear valence orbitals are s, p - states at threshold (pairing anti-halo effect). Examples of situations of this mechanism

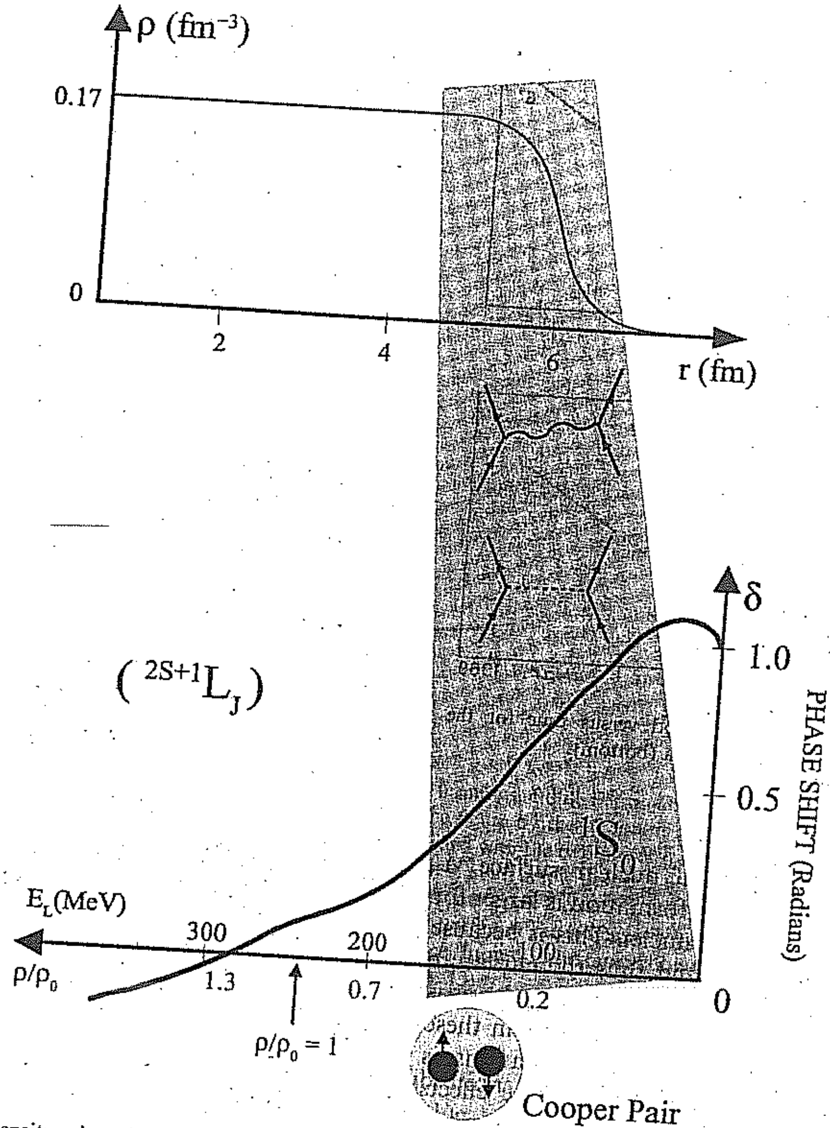

Fig. 13. (top) Nuclear density ρ in units of fm^{-3} (where fm $\equiv 10^{-13}$ cm), plotted as a function of the distance r (in units of fm) from the centre of the nucleus. Saturation density correspond to ≈ 0.17 fm^{-3}, equivalent to 2.8×10^{14} g/cm^3. Because of the short range of the nuclear force, the strong force, the nuclear density changes from 90% of saturation density to 10% within 0.65 fm, i.e. within the nuclear diffusivity. (bottom) Phase parameter associated with the elastic scattering of two nucleons moving in states of time reversal, so called $^1S_0$ phase shift, in keeping with the fact that the system is in a singlet state of spin zero. The solution of the Schrödinger equation describing the elastic scattering of a nucleon from a scattering centre (in this case another nucleon) is, at large distances from the scattering centre a superposition of the incoming wave and of the outgoing, scattering wave. The interaction of the incoming particle with the target particle changes only the amplitude of the outgoing wave. This amplitude can be written in terms of a real phase shift—or scattering phase—δ. Positive values of δ implies an attractive interaction, negative a repulsive one. For low relative velocities (kinetic energies E_L), i.e. around the nuclear surface where the density is low, the $^1S_0$ phase shift arizing from the exchange of mesons (like for example pions, represented by an horizontal dotted red line) between nucleons (represented by upward pointing arrowed lines) is attractive. This mechanism provides about half of the glue to nucleons moving in time reversal states to form Cooper pairs. These pairs behaves like boson and eventually condense in a single quantal state leading to nuclear superfluidity. Cooper pair formation is further assisted by the exchange of collective surface vibrations (green wavy curve in the scattering process) between the members of the pair.

type are provided by $N=6$ (parity in- $\boxed{box 4}$
version) isotones. In particular, by ^{11}Li (2), in which
case the strongly renormalized $s_{1/2}$ and $p_{1/2}$
valence orbitals are a virtual and a resonant
state lying at ≈ 0.1 and 0.6 MeV in the
continuum, respectively. In keeping with
the fact that the binding provided to
a pair of fermions moving in time reversal
states by a contact pairing interaction
(δ-force) is (cf. e.g. Eq. (2.12) Brink and
Broglia (2005)) $E_0 = -(2j+1)/2\, V_0\, I(j) \approx -\frac{(2j+1)}{2} V_0 \frac{3}{R^3}$,
the ratio

$$r = \frac{2}{(2j+1)}\left(\frac{R_0}{R}\right)^3,$$

where $R_0 = 1.2 A^{1/3}$ fm $= 2.7$ fm $(A=11)$, and
$R = \sqrt{\frac{5}{3}} \langle r^2 \rangle^{1/2}_{^{11}Li} = \sqrt{\frac{5}{3}}\ 3.74$ fm $= 4.6$ fm are the
radius of a stable nucleus of mass $A=11$
(systematics), while R is the measured
one, while j is the angular momentum
representative for a nucleus of mass $A=11$
($j \sim k_F R_0 \approx 3$-4), one obtains $r = 0.06$.
Making use of the multipole expansion
of a general interaction

$$v(|\vec{r}_1 - \vec{r}_2|) = \sum_\lambda V_\lambda(r_1, r_2)\, P_\lambda(\cos\theta_{12}),$$

Because the function P_λ drops from its
maximum at $\theta_{12} = 0$ in an angular distance
$1/\lambda$, particles 1 and 2 interact through the

component λ of the force, only $\boxed{\text{Box 4}}$ (3)
if $r_{12} = |\vec{r}_1 - \vec{r}_2| < R/\lambda$, where R is the mean value of the radii $\vec{r}_1$ and $\vec{r}_2$. Thus, as λ increases, the effective force range decreases. For a force of range much greater than the nuclear size, only the $\lambda = 0$ term is important. At the other extreme, a δ-function force has coefficients $V_\lambda(r_1, r_2)$ $\left(= \frac{(2\lambda+1)}{4\pi r_1^2}\delta(r_1 - r_2)\right)$ that increase with λ.

In the case of $^{11}Li(gs)$ we are thus forced to accept the need for a long range, low λ pairing interaction, as responsible for the binding of the dineutron, halo Cooper pair to the ^{9}Li core. This is equivalent to saying, an induced pairing interaction arising from the exchange of vibrations with low λ-value.

Boostrap Cooper pair binding

Within the s, p subspace, the most natural long wavelength vibration is the dipole mode. From systematics, the centroid of these vibrations is $\hbar\omega_{GDR} \approx 100\,MeV/R$, R being the nuclear radius. Thus, in the case of ^{11}Li, one expects the centroid of the Giant Dipole Resonance carrying $\approx 100\%$ of the energy weighted sum rule (EWSR) at $\hbar\omega_{GDR} \approx 100\,MeV/2.7 \approx 37\,MeV$. Now, such a high frequency mode can hardly be expected to give rise to anything, but polarization effects. On the other hand, there exists experimental evidence which testifies to the presence of a rather sharp dipole state with centroid at $\approx 1\,MeV$ and carry $\approx 10\%$ of the

EWSR. The existence of this $\boxed{\text{box 4}}$ (4)

"pigmy resonance" which can be viewed as a simple consequence of the existence of a low-lying particle hole state associated with the transition $s_{1/2} \rightarrow p_{1/2}$, arguably, testifies to the coexistence of two states with rather different radii in the ground state*). One, closely connected with the compact (≈ 2.7 fm) ^{9}Li core, the second with the diffuse halo (≈ 4.6 fm). Because the overlap between them is smal ($\approx (2.7/4.6)^3 \approx 0.2$), one can posit that a bona fide dipole pigmy resonance is a GDR based on an exotic, unusually extended state as compared to systematics ($A \approx (4.6/1.2)^3 \approx 60$), i.e. to a system with an effective A mass number about 5 time than predicted by systematics**)

Let us try to shed some light on these issues. Making use of of the ralation $\langle r^2\rangle^{1/2} \approx (3/5)^{1/2} R$ between mean square radius and radius, one may write

$$\langle r^2\rangle_{^{11}Li} \approx \frac{3}{5} R_{eff}^2 (^{11}Li).$$

Furthermore, the pigmy dipole resonance may be built not only on the ~~large~~ extended component of the ground state as in ^{11}Li but also on excite ~~states~~ like e.g. ^{12}Be (see Fig. 2.)

*) This is reminiscent of the deformation coexistence found in e.g. ^{16}O, ^{40}Ca ground ~~state~~ and, recently in - - - -

**) Within this context the dipole strength fond at ≈ 10 MeV in neutron skin rich nuclei can hardly be consider pigmy resonance, but the long tail of the GDR.

with

$$R_{eff}(^{11}Li) = \left(\frac{9}{11} R_0^2(^9Li) + \frac{2}{11}\left(\frac{\xi}{2}\right)^2\right),$$

where

$$R_0(^9Li) = 2.5 \text{ fm}$$

is the ^9Li radius ($R_0 = r_0 A^{1/3}$, $r_0 = 1.2$ fm), where ξ is the correlation length of the Cooper pair neutron halo. An estimate of this quantity is provided by the relation

$$\xi = \frac{\hbar v_F}{2 E_{corr}} \approx 20 \text{ fm},$$

in keeping with the fact that in ^{11}Li, $(v_F/c) \approx 0.1$ and $E_{corr} \approx 0.5$ MeV. Consequently, $\langle r^2 \rangle^{1/2}_{^{11}Li} \approx 3.74$ fm ($R_{eff}(^{11}Li) \approx 4.83$ fm), in overall agreement with the experimental value $\langle r^2 \rangle^{1/2}_{^{11}Li} = 3.55 \pm 0.1$ fm (Kobayashi et al., 1989).

We now proceed to the calculation of the centroid of the dipole pigmy resonance of ^{11}Li. Making use of the dispersion relation given in Eq. (3.30) p. 55 of Bortignon et al, 1998, and of the fact that $\varepsilon_{1/2} - \varepsilon_{1/2} = \varepsilon_{p1/2} - \varepsilon_{s1/2}$ ≈ 0.5 MeV (see Fig. 11.1 p. 264 Brink and Broglia (2010)),

Brink D. M and R. A. Broglia (2010) Nuclear Superfluidity, Cambridge University Press, Cambridge,
Kobayashi .... (1989) Phys. Lett. B 332, 51)
Bortignon, P.F., A. Bracco and R. A. Broglia (1998) Giant Resonances, Harwood Academic Publishers, Amsterdam.

and that the EWSR associated with the ^{11}Li pigmy resonance is $\approx 10\%$ of the total Thomas-Reiche-Kuhn sum rule one can write,

$$0.1\frac{\hbar^2 A}{2M} = \frac{1}{K_1}\left[(0.5\,\mathrm{MeV})^2 - (\hbar\omega_{pigmy})^2\right],$$

and thus

$$(\hbar\omega_{pigmy})^2 = (0.5\,\mathrm{MeV})^2 - 0.1\frac{\hbar^2 A}{2M}K_1,$$

where (see Bortignon et al (1998))

$$K_1 = -\frac{5V_1}{A(5/2)^2}\left(\frac{2}{11}\right) = -\frac{125\,\mathrm{MeV}}{A\times 100\,\mathrm{fm}^2}\left(\frac{2}{11}\right) \approx -\frac{2.5}{A^2}\,\mathrm{fm}^{-2}\,\mathrm{MeV},$$

the ratio in parenthesis reflecting ~~the fact that~~ only 2 out of 11 nucleons, slosh back and forth in an extended configuration with little overlap with the other nucleons. One then obtains,

$$-0.1\frac{\hbar^2 A}{2M}K_1 = 0.1\times 20\,\mathrm{MeV\,fm}^2\,A\times\frac{2.5}{A^2}\,\mathrm{fm}^{-2}\,\mathrm{MeV}$$
$$\approx 0.45\,\mathrm{MeV} \approx (0.7\,\mathrm{MeV})^2$$

consequently

$$\hbar\omega_{pigmy} = \sqrt{(0.5)^2+(0.7)^2}\,\mathrm{MeV} \approx 1\,\mathrm{MeV},$$

in overall agreement with the experimental findings (Zinser et al, 1997). It is of notice that the centroid of the pigmy resonance calculated in the RPA with the help of a separable interaction is $\approx (0.8\,\mathrm{MeV} + 2.0\,\mathrm{MeV})/2 \approx 1.4\,\mathrm{MeV}$ (see Fig. 11.3(a) p. 269, Brink and Broglia, 2010).

Let us now estimate the binding which the exchange of the pigmy resonance between two neutron of the Cooper pair halo of ^{11}Li can provide

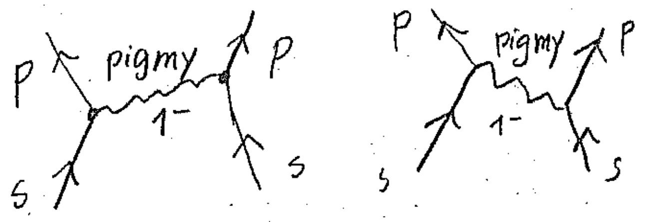

The associated particle vibration coupling $\Lambda = \left(\partial W(E)/\partial E\big|_{\hbar\omega_{pigmy}}\right)^{-1/2}$, where $W(E)$ is the dispersion relation used to determine $\hbar\omega_{pigmy}$ (cf. e.g. Brink and Broglia Eq. (8.42) p. 189; (note the use of a dimensionless dipole single particle field $F'_{dim} = F/\langle r^2\rangle_{^{11}Li}$)

$$W(E) = \sum_{\nu_k \nu_i} \frac{2(\epsilon_k - \epsilon_i)\,|\langle \tilde{i}|F/\langle r^2\rangle_{^{11}Li}|k\rangle|^2}{(\epsilon_k - \epsilon_i)^2 - E^2}$$

Zinser et al 1997 Nucl. Phys. A619, 151.

One then obtains

$$\Lambda^2 = \left\{ 2\hbar\omega_{pigmy} \frac{0.1(TRK)/\langle r^2\rangle_{^{11}Li}}{[(\varepsilon_{p1/2}-\varepsilon_{s1/2})^2-(\hbar\omega_{pigmy})^2]^2} \right\}^{-1}$$

$$= \left\{ 2\,\mathrm{MeV} \frac{0.1(\hbar^2 A/2M)(1/\langle r^2\rangle_{^{11}Li})}{[(0.5)^2-(1\,\mathrm{MeV})^2]^2\,\mathrm{MeV}^4} \right\}^{-1}$$

$$= \left(\frac{0.75}{1.57}\right)^2 = 0.48\,\mathrm{MeV}^2$$

leading to $\Lambda = 0.7$ MeV. The value of induced interaction matrix element is then given by

$$M_{ind} = -\frac{\Lambda^2}{\hbar\omega_{pigmy}} = -0.5\,\mathrm{MeV},$$

and the same contribution for the other time ordering. Assuming the halo neutrons to spend the same amount of time in the $|s_{1/2}^2(0)\rangle$ ($\varepsilon_{s1/2}=0.1$ MeV) than in the $|p_{1/2}^2(0)\rangle$ ($\varepsilon_{p1/2}=0.6$ MeV) configuration, the correlation energy is $E_{corr} = |2(\varepsilon_{s1/2}+\varepsilon_{p1/2})/2 + 2M_{ind}| = 0.3$ MeV, in overall agreement with the findings (0.380 MeV, reference).

2.24 MeV

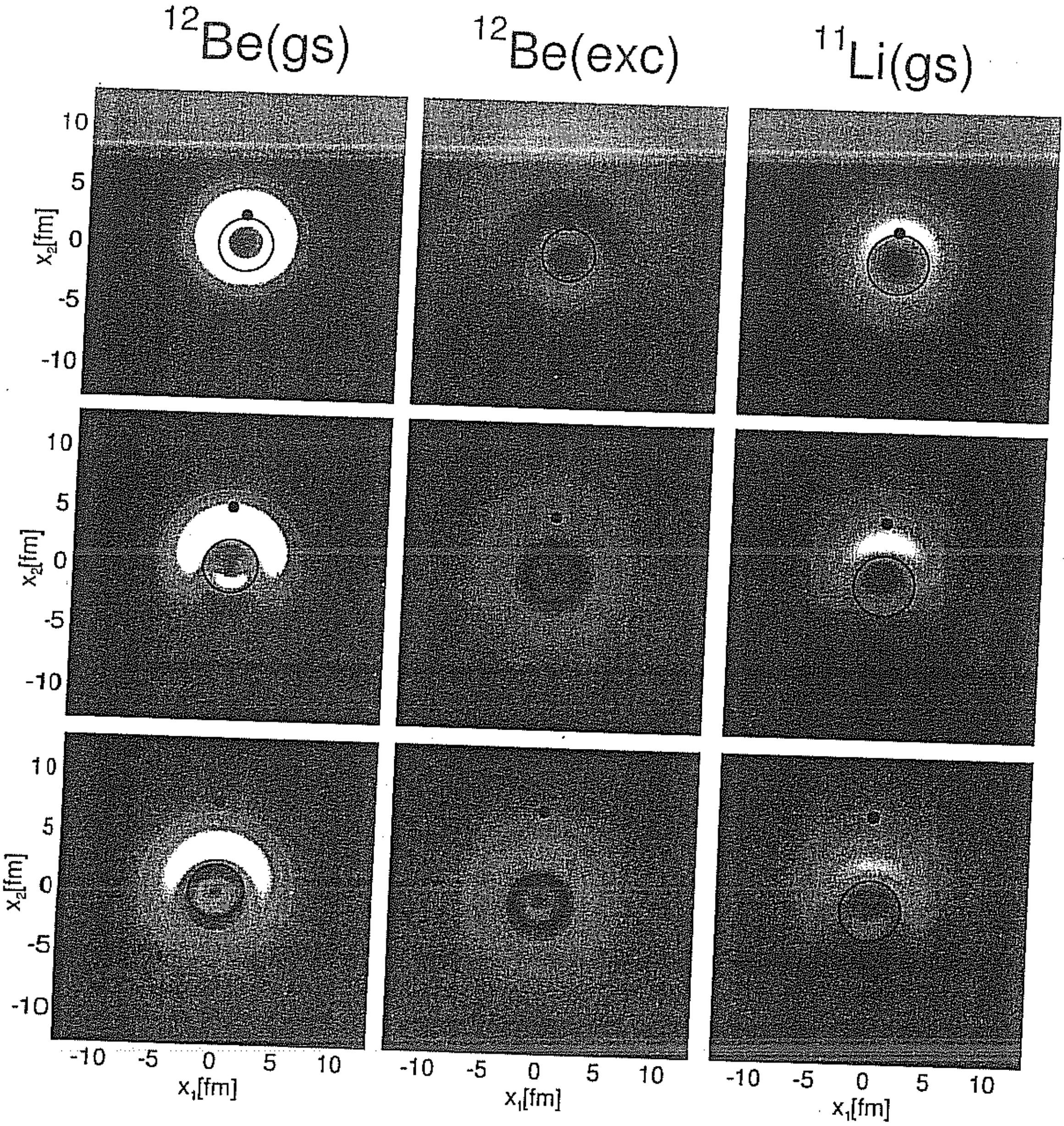

$$|0\rangle_\nu = |0\rangle + \alpha|(p,s)_{1^-} \otimes 1^-;0\rangle + \beta|(s,d)_{2^+} \otimes 2^+;0\rangle + \gamma|(p,d)_{3^-} \otimes 3^-;0\rangle$$

$$|0\rangle_\nu = a|s^2(0)\rangle + b|p^2(0)\rangle + c|d^2(0)\rangle$$

	^{11}Li(gs)	^{12}Be(gs)	^{12}Be(exc)
α	0.7	0.10	0.08
β	0.1	0.30	-0.39
γ	–	0.37	-0.1
a	0.45	0.37	0.89
b	0.55	0.50	0.17
c	0.04	0.60	0.19

$\boxed{\text{exotic decay}}$ →

← pigmy resonance in Pb

$s^2(0)$

at threshold